

EVAPORATION DECAY OF ORGANIC ICE NUCLEUS PARTICLES*

H. R. Vasquez** and N. Fukuta
 Department of Meteorology, University of Utah, Salt Lake City, Utah 84112

Abstract. Evaporation rates have been determined for two organic ice nucleus particles: 1,5-Dihydroxynaphthalene and metaldehyde aerosols, produced by powder vaporization-condensation method and by vapor activation method, respectively. The aerosols are injected into a large smoke chamber inside a walk-in environmental room and allowed to evaporate under dry conditions at different temperatures. The decay rates of aerosols are determined in a mixing chamber at -15 C with intermittent sampling at predetermined time intervals. The aerosol concentration losses are compared with cumulative size distributions, and assuming that the decay proceeds from smaller sizes, lifetimes of particles for different temperatures are determined as a function of minimum size. Metaldehyde particles less than 0.6 μm in diameter decay within 20 minutes at temperature as cold as -20 C, and 1,5-dihydroxynaphthalene particles within several hours, if particle diameters are smaller than 0.2 μm at the same temperature. These data are expected to provide the basis for estimating, as well as minimizing, the extent of possible downwind and environmental contamination through use of these organic ice nucleants.

1. INTRODUCTION

For cloud seeding, choice of ice nucleant characteristics and proper application of the nucleant in terms of space and time, if seedability of the cloud is established, will provide an opportunity to improve the seeding technique.

A widely used ice nucleant, silver iodide (AgI), has features attributable to its physico-chemical characteristics. The high efficiency of ice nucleus particle production per gram of the compound is related to its relatively high melting point, or latent heat of condensation. The large condensation heat gives a sharp vapor pressure drop during cooling of smoke production, leading to generation of high supersaturation and resulting in production of a large number of small particles. However, the same physico-chemical characteristic leads to extremely low vapor pressure of the compound, virtually undetectable under cloud seeding temperatures. Naturally, AgI particles as small as hundredths of one micron are thus stable against possible evaporation loss.

The lifetime of a small particle before evaporation, t_e , is proportional to the square of the diameter d , if the effects of accommodation coefficients can be ignored (Fukuta and Walter, 1970), or

$$t_e \propto d^2. \quad (1)$$

Small aerosol particles of a compound which appears stable in powder form at room temperature can evaporate surprisingly fast if the vapor pressure of the compound is not vanishingly small. Silver iodide does not belong to this category and the non-evaporating nature of AgI particles permits its application from a warm or dry zone, or from a place remote to the target area, so that eddy diffusion of

the particles into sufficiently large cloud volume can take place effectively. In this regard AgI has advantages over homogeneous ice nucleants such as dry ice. This stability of AgI particles in air, however, may lead to their survival and let them work later in unwanted areas.

Increasing evidence is available that the effects of cloud seeding operations reach beyond the geographic areas for which they are intended (Elliot and Brown, 1971; Grant and Mulvey, 1971; Warburton, 1971). The low active number of AgI particles at warm temperatures (Garvey, 1975) is often compensated by introducing a large number of nuclei into the cloud, usually resulting in an overseeded or glaciated condition at high altitudes. Large number of unactivated nuclei may drift downwind together with millions of small ice crystals. Silver, in such cases, has been detected in precipitation by atomic absorption and thermal neutron activation analysis (Warburton and Young, 1968). Grant and Mulvey (1971) documented downwind phenomena in eastern Colorado. During the Climax and Wolf Creek pass projects, AgI drifted 130 miles (215 km) downwind and underwent lee wave subsidence into upslope cloud system. Freshly fallen snow on 29 unseeded days and 12 seeded days, analyzed by the atomic absorption technique, showed that cloud seeding produced five times the normal background silver concentrations present in the atmosphere.

Small particles of a given organic nucleant can evaporate to lose their activity, depending primarily on particle size and air temperature (Fukuta et al., 1966). In past studies (Fukuta, 1963, 1972 and 1974; Fukuta et al., 1966; Fukuta and Paik, 1976; Fukuta et al., 1976; Fukuta et al., 1977; Schaller and Fukuta, 1979), two organic ice nucleants showed promise for weather modification and were subsequently tested: metaldehyde (MA) and 1,5-dihydroxynaphthalene (DN). Apart from their cost advantages over AgI (Fukuta et al., 1977), the organic nucleants are more attractive as far as possible environmental effects are concerned, although AgI does not seem to pose any serious danger to the environment under normal cloud seeding operations

* Paper presented at the Eighth Conference on Inadvertent and Planned Weather Modification, Reno, Nevada, 5-7 October 1981.

** Current affiliation: Center Weather Service Unit, FAA, ARTCC, 2555 E. Ave. P., Palmdale, CA 93350.

(Cooper and Jolly, 1970; Teller, 1972). However, care must be exercised when massive seeding dosages are anticipated (Sokal and Klein, 1975). Fresh water fish are known to be sensitive to pollutants (Table 1).

Table 1

Changes in reproductive and mortality rates for small fish exposed to seeding agent chemicals (Church et al., 1975).*

Aquaria Age (week)	No Seeding Agent	Seeding Agents (mg/l)									
		MA			PG**			DN		AgI	
		1	10	100	1	10	100	1	10	1	10
1	8	4	3	2	4	3	2	4	3	4	2
2	8	4	3	2	3+	3	2	4	4	2	2
3	7+	4	4	3+	3	4	2	4+	4	4	0
4	8+	4+	4+	3	4	4	3	4	3+	3	2
5	7+	3+	4	3	4	3	2	3+	4	3	2
Total Fish Loss	2	1	2	7	2	3	9	1	2	4	12
Total Fish Hatch	3	2	1	1	1	0	0	2	1	0	0

* Numbers are fish surviving each week of aquaria life. Plus signs represent delivery of young by one gravid female.

** Phloroglucinol.

Considering these advantages of organic ice nucleants, if evaporation of the smoke particles could be programmed to occur at a proper time after the ice nucleation period in the cloud, a new basis would be provided for selecting seeding materials. For this reason the evaporation decay of ice nucleating ability was investigated experimentally for MA and DN smokes as a function of size and temperature.

2. GENERATION AND SIZE DISTRIBUTION OF ORGANIC SMOKE PARTICLES

To investigate the activity decay of organic smoke particles by evaporation, the particles must be generated properly and their size distribution determined.

2.1 1,5-Dihydroxynaphthalene

A simple aerosol generation method was used: a soldering iron with its heating element wound with one-eighth inch (3.2 mm) ID copper tubing with a syringe attached to it by a rubber tube. To generate the smoke, a small amount of DN powder is placed into one end of the copper tubing and blown by the syringe through the heated copper coil. The powder vaporizes in the coil, producing a high concentration of needed smoke particles at the exit.

Particle evaporation rate is highly dependent upon size and temperature, so size distribution must be determined. Particle sizes were determined by measuring their fall speed under dark field illumination in an ultra-microscope (Green and Lane, 1964). Aerosol sizes greater than 1 μm in diameter can then be estimated through Stokes' fall velocity equation (Hesketh, 1977),

$$v = d^2 g \Delta\rho / 18 \eta, \quad (2)$$

where d is the particle diameter, g the gravitatio-

nal acceleration, $\Delta\rho$ the density difference between particle and air, and η the viscosity of air. When the particle diameter is smaller than 1 μm , Cunningham's correction factor must be used in Stokes' equation:

$$C = 1 + 2\lambda A/d, \quad (3)$$

here λ is the mean free path of air molecules, and A a constant close to unity. Figure 1 shows the

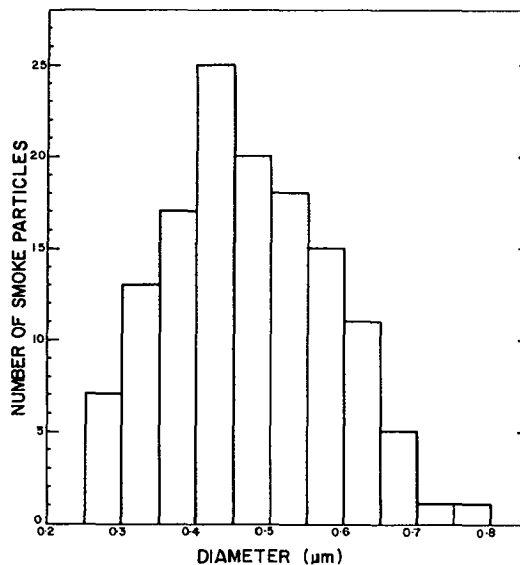


Fig. 1. Stokes-Cunningham size distribution of 1,5-dihydroxynaphthalene smoke particles.

Stokes-Cunningham size distribution obtained for DN particles. The average particle diameter of DN smoke is 0.41 μm .

The effective DN nuclei concentration per gram of material produced by the present smoke generation device was estimated. The temperature spectrum of smoke particle activity helps us determine the most efficient temperature setting for an ice nucleation test in the mixing chamber. This estimation also helps determine a smoke dilution factor, or number of particles per cm^3 , necessary to avoid saturation of the air environment with DN vapor after evaporation. The concentration of organic particles should be low enough so that they can evaporate freely in unsaturated air. To make smoke, a known amount (about 2 mg) of DN powder was put into the generator and injected through the heated copper tube into Box 1. A portion of the aerosol was then extracted and diluted again in Box 2. Then 10 cm^3 of the diluted sample was taken from Box 2 and tested in the mixing chamber. An effective nuclei number of $10^{12}/\text{g}$ was determined at both -15 and -20 C, but dropped to $10^9/\text{g}$ at -10 C. A temperature setting of -15 C was subsequently selected for the mixing chamber experiments.

2.2 Metaldehyde

Unlike DN, MA aerosol particles cannot be produced effectively by vaporization through the handheld aerosol generator. When MA and water are boiled together and the vapor mixture quenched, water vapor condensing onto the formed MA particles nucleates a large number of ice crystals. This technique, called "Vapor Activation" (Fukuta, 1968), is

applied to the smoke particle generation. The smoke generating device consists of a 1 l Erlenmeyer flask containing MA and water, a rubber stopper and a copper tubed orifice which vents the vapors, and a rubber hose connected to a 1.5 l syringe. The smoke generation method is similar to that for DN. After boiling and filling the flask with the vapor mixture, the syringe air is pushed into it, purging the vapor mixture into Box 1.

The MA aerosol particle size was determined in the same manner as for DN, from fall velocity measurement and the Stokes-Cunningham equation. The average particle diameter of MA is 0.79 μm (Fig. 2).

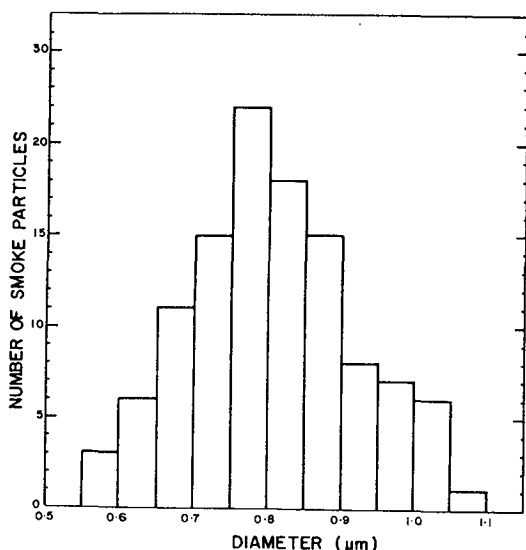


Fig. 2. Stokes-Cunningham size distribution for vapor-activated metaldehyde smoke particles.

Small particles, microscopically visible, disappeared several minutes after injection into the observation cell, as a result of evaporation. The number of ice crystals produced per gram of MA by vapor-activation method is 2×10^{13} at -20 C and 5×10^{11} at -10 C (Fukuta *et al.*, 1970).

To assure free evaporation of MA particles during the experiments, preliminary runs were made using the mixing chamber at a few environmental temperatures. Computations confirmed that the evaporation decay was sufficiently faster than particle settling and other losses.

3. EXPERIMENTAL

3.1 Evaporation

A 6 m^3 aerosol chamber was constructed of masonite for the evaporation experiments. A small, electrically driven fan stirs the air containing the aerosol particles. Several holes are bored on the side for application of a thermometer, thermister unit, microscope lamp, and laser for optical detection of ice crystals, for injecting steam for ice crystal growth and two large holes for post clean-up operations. A service door cut into the bottom allowed insertion of formvar covered glass slides for ice crystal collection and replication.

A walk-in environmental room 3.3 x 2.7 x 2.2 m^3

holds the aerosol chamber under controlled temperatures ranging from 50.5 down to -15 C. The environmental room was originally designed for low temperature operations, and to maintain a constant high temperature a portable heater was installed with an Omega Engineering thermoregulator and thermistor.

The mixing chamber used for this study was a 10-l copper cylinder held in a large temperature-controlled circulating bath. It has a lid, a cellulose acetate tube filled with warm water for moisture source, and a sugar solution. The interior of the chamber is painted black and a glycerine solution coats the walls to avoid ice crystal fall from them. In the lid, made of plexiglass, a small hole provides an entrance for smoke particles and a large hole serves as a handle and support for the moisture source, a cellulose acetate semipermeable membrane tube filled with warm water. In measurements, this tube is warmed in a water-filled beaker to 50 C, and subsequently attached to the mixing chamber lid several minutes before aerosol injection. Vapor produced by the membrane provides supercooled fog needed for contact-freezing and deposition ice nucleation measurements.

A supercooled sugar solution tray, painted black, is placed on the floor of the mixing chamber which receives nucleated ice crystals. To count all the nucleated ice crystals for a sufficiently long period of time, the ice crystal growth rate in the solution has to be controlled through adjustment of the concentration. For this reason, the growth rate of ice crystals in the sugar solution was determined as a function of the specific gravity at various temperatures (Fig. 3).

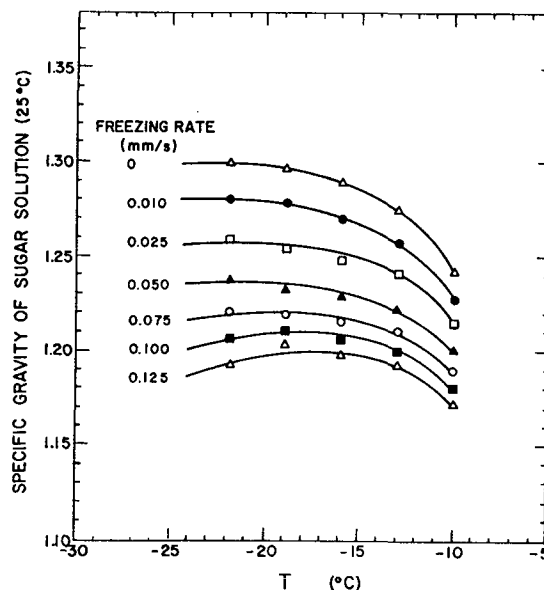


Fig. 3. Ice crystal growth rates as a function of temperature and specific gravity of sugar solution.

The study involves evaporation measurements of organic aerosols held in a large smoke box under different temperatures. Smoke samples in the large smoke chamber are periodically withdrawn and introduced into a mixing chamber where particle activity loss is determined as a function of time.

Aerosol particles can be lost by mechanisms

other than evaporation, such as coagulation, sedimentation, and sticking to the walls. To determine the evaporation loss of aerosol particles, contributions from other mechanisms were estimated theoretically.

3.2 Other Losses

The coagulation rate of an aerosol containing n particles per cm^3 is given by

$$\frac{dn}{dt} = -Kn^2, \quad (4)$$

where t is the time and K the coagulation constant (Green and Lane, 1964). In a series of experiments to determine coagulation rates and constants as a function of particle number concentration, size, turbulence, and chamber size, Gillespie and Langstroth (1951) found the coagulation constant to be little affected by turbulent motions less than 40 m/min through a given volume. Experiments using a similar size, light mixing, and relatively low particle numbers, produced $K = 0.4 \times 10^{-8} \text{ cm}^3/\text{min}$. Using these data, concentration loss was determined to be very small: 99.9% of the particles remain after 6 hours, assuming an initial aerosol population of 10^3 per cm^3 . Particle concentration for both DN and MA were estimated to vary between 1 and 3 per cm^3 ; in this regard, their losses by coagulation in our experimental periods were negligible.

Gravitational fallout of particles in the chamber is also important because it reduces the particle number available for measurements. The rate of particle deposition while being stirred is given by (Green and Lane, 1964)

$$n = n_0 \exp(-v t / h), \quad (5)$$

where n_0 is the initial particle concentration, v the average particle terminal velocity, t the time, and h the chamber height. Concentration loss due to gravitational fallout under our conditions was negligible, with 99% remaining after 6 hours.

A turbulent medium inside a chamber will continually bring air into contact with its surfaces, and all particles striking the walls will stick to them, reducing aerosol concentrations. The chance that a particle will strike the surface is proportional to particle number concentration and the rate of concentration loss can be represented by the surface loss equation,

$$n = n_0 \exp(-B t), \quad (6)$$

where B is the particle surface loss rate constant, affected by size of particles, turbulence, and size of chamber. Smaller particles favor deflection with air currents near the surfaces, while momentum of large particles influences surface collisions and results in a high loss rate. According to Gillespie and Langstroth (1951), under our experimental conditions, $B = 0.4 \times 10^3 \text{ min}^{-1}$. Surface concentration losses were therefore calculated to be about 10% within 4 hours. However, with our small DN and MA concentrations and with nearly total evaporation during this period, losses were considered negligible.

Another anticipated problem was whether particle evaporation would be hindered through the possible chamber air saturation with the vapor of the organic compound during the evaporation measurement.

To avoid this problem, vapor density was computed as a function of temperature from DN and MA vapor pressure values measured in our laboratory (Fig. 4).

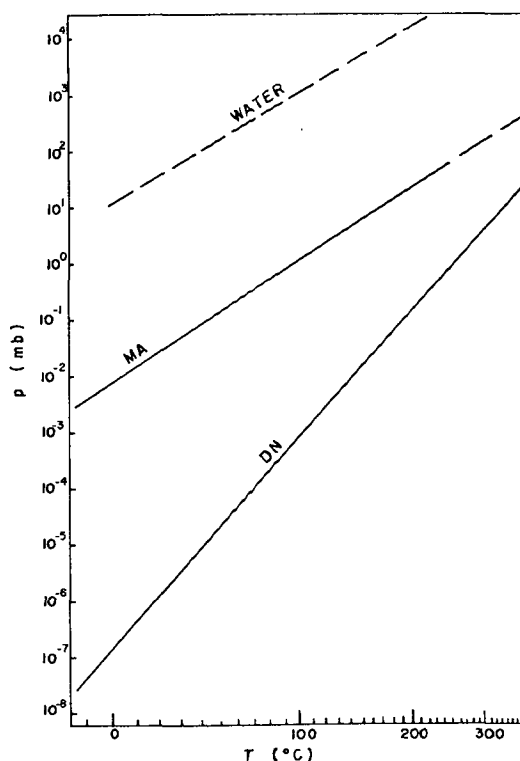


Fig. 4. Saturation vapor pressures of 1,5-dihydroxynaphthalene, metaldehyde and water.

From the average organic particle diameter and density, particle mass was estimated, and compared to the vapor density to indicate the number of particles required to saturate one cubic centimeter of air as a function of temperature. Particle number concentrations used in our experiments were 1 to 3 per cm^3 , far below the limits.

4. EXPERIMENTAL RESULTS

4.1 1,5-Dihydroxynaphthalene

The first step in our evaporation measurement was to inject a predetermined number of organic smoke particles into the large smoke chamber, where the particles were continuously stirred and contained for several hours at a given temperature, while evaporation tests were performed. Initially, we were to expose this organic smoke to sub-freezing temperatures and monitor the decay rate for 5 to 10 hours, but because of the slow evaporation rate of the DN smoke particles, we decided to speed up the decay process by heating the chamber. A subsequent extrapolation scheme was used to determine the decay rates at temperatures more representative of the real atmosphere. Four temperatures were used; 35.5, 40.5, 45.5, and 50.5 C.

After the organic smoke had been injected into the large aerosol chamber, samples were taken at predetermined intervals and tested in the mixing chamber. Samples were drawn ten minutes after initial injection and thereafter every half-an-hour for 3 to 6 hours. One liter aerosol samples were withdrawn periodically with the syringe and slowly injected into the supercooled fog held at -15 C.

After injection, a waiting period of five minutes allowed ice crystals formed on the DN nuclei to develop into visible white spots in the supercooled sugar solution. Measurements were made every other day due to the necessary chamber clean-up process, by heating to evaporate all existing particles and to vent out the vapor during the intervening day.

Our experiments consistently showed a decrease in the number of collected ice crystals with time, indicating that evaporation was indeed taking place within the large aerosol chamber. After a series of experiments at each desired temperature level was completed, data were plotted immediately to check the evaporation trend. Figures 5 through 8 co-

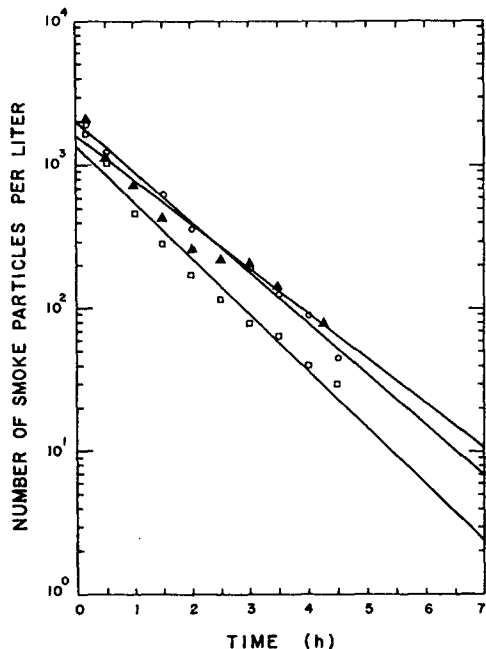


Fig. 5. Evaporation decay for 1,5-dihydroxynaphthalene smoke particles determined at 35.5 C.

mpare the differences in evaporation rates for particle concentrations determined at four temperature levels. As expected the slowest concentration loss was observed at 35.5 C. With increasing temperature, the decay slope steepened.

The decay curves were fairly easy to determine, with the exception of that at 50.5 C, where evaporation was so rapid that the number of smoke particles dropped beyond the detection limit of the chamber. However, because the injection procedure was identical to the runs at other temperatures, initial ice crystal concentration could be inferred, and using small number of crystals experimentally detected, a concentration loss curve was estimated. The 50.5 C decay curve seemed to follow the same pattern as others, illustrated by the near linear concentration loss slope profile given in Fig. 9. Concentration losses can be calculated for temperature levels more realistic to our atmosphere by using the empirical equation

$$n = n_0 \exp [-b t \exp (m T)], \quad (7)$$

where $b = 0.0007$, $m = -0.132$ and T the temperature.

4.2 Metaldehyde

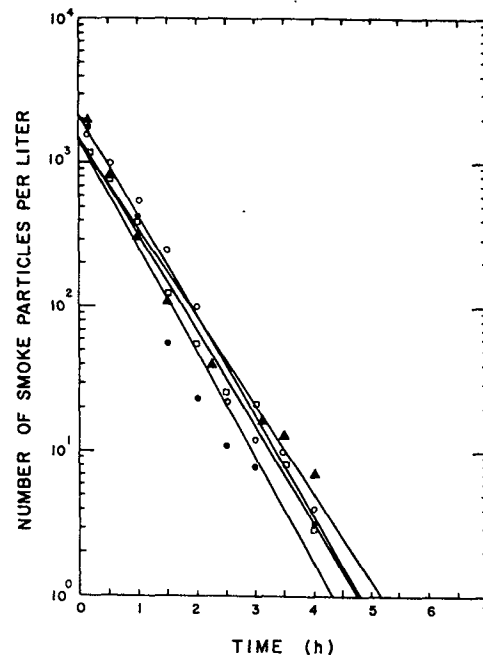


Fig. 6. Evaporation decay for 1,5-dihydroxynaphthalene smoke particles determined at 40.5 C.

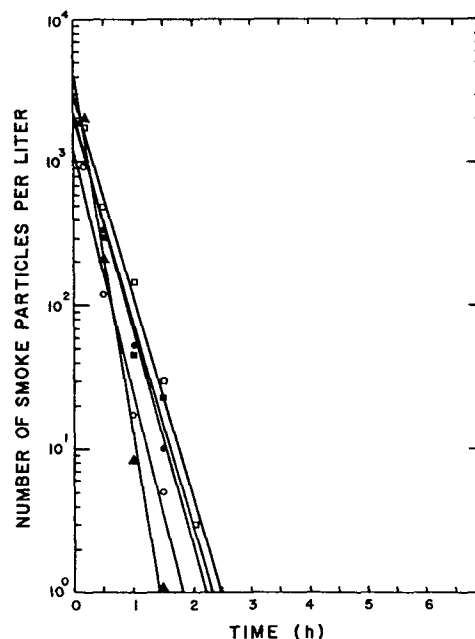


Fig. 7. Evaporation decay for 1,5-dihydroxynaphthalene smoke particles determined at 45.5 C.

The measurement technique for evaporative concentration loss for MA was similar to that for DN, except for the method of particle generation, which reflects the difference in material characteristics. Vapor-activated MA (Section 2.2) was dispensed into the large chamber to produce a high concentration of ice crystals, which subsequently sublimated, exposing the small MA particles. To assure that the formed ice crystals sublimate, a dry environment was created in the chamber through heating and injection of compressed air, with ventilation to

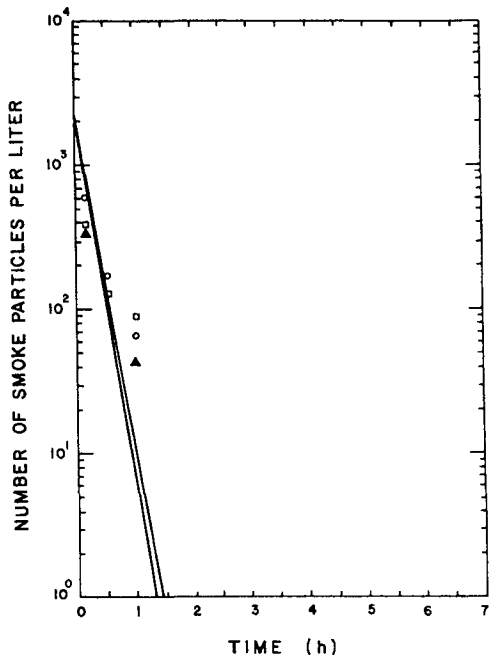


Fig. 8. Evaporation decay for 1,5-dihydroxynaphthalene smoke particles determined at 50.5 C.

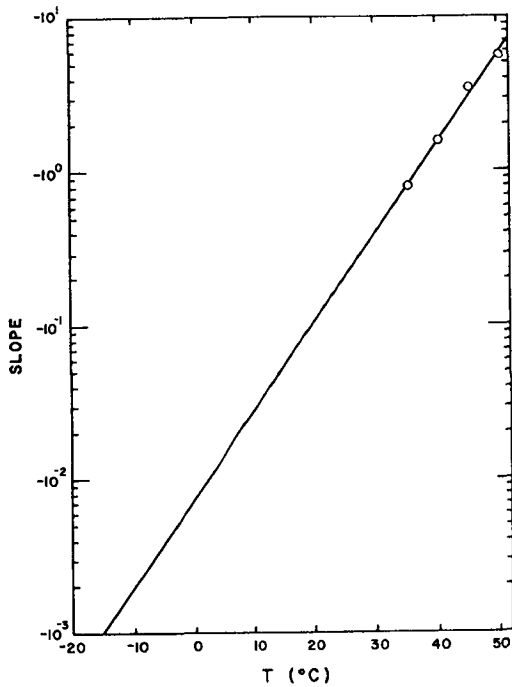


Fig. 9. Slopes of evaporation curves for 1,5-dihydroxynaphthalene particles plotted as a function of temperature.

lower the amount of water vapor inside the chamber. Ice crystal sublimation was confirmed by lack of visible signs of ice crystals in a light beam from a laser or microscope lamp directed into the chamber ten minutes after vapor activation.

The particles thus produced were continually stirred throughout the entire experimental run at subfreezing temperatures of -5, -10, and -15 C.

Samples were drawn as described in Section 4.1, and results were analyzed immediately to check the evaporation trend. Figures 10 through 12 compare the

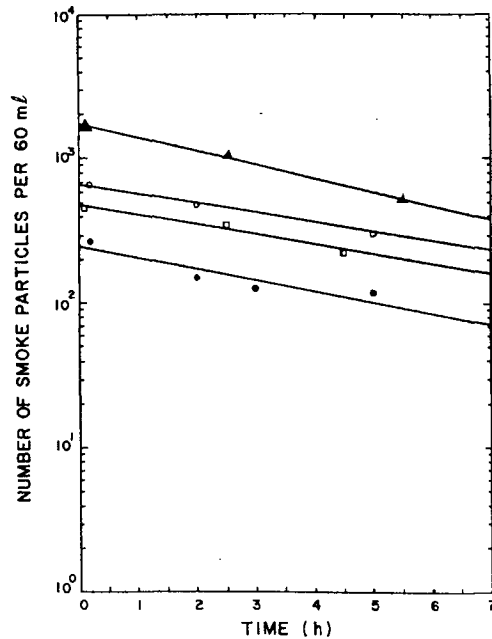


Fig. 10. Evaporation decay for metaldehyde smoke particles determined at -15 C.

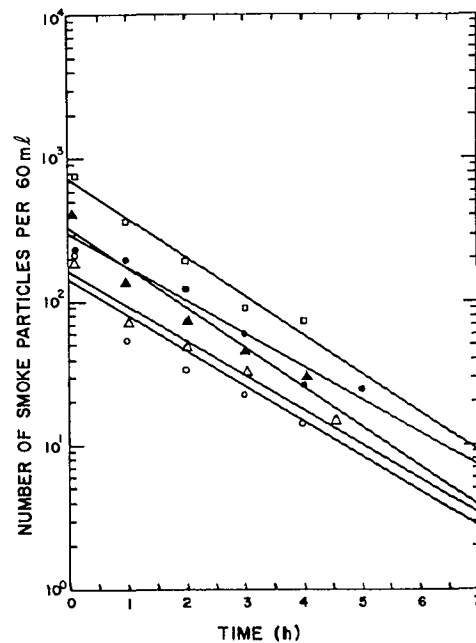


Fig. 11. Evaporation decay for metaldehyde smoke particles determined at -10 C.

differences in particle concentration decay rates for the three temperatures used. As expected, -15 C data showed the slowest evaporation rate, while concentration losses were fastest at -5 C. The number concentrations at $t = 0$ did not show good reproducibility as seen in the graphs; however, the decay slopes were consistent.

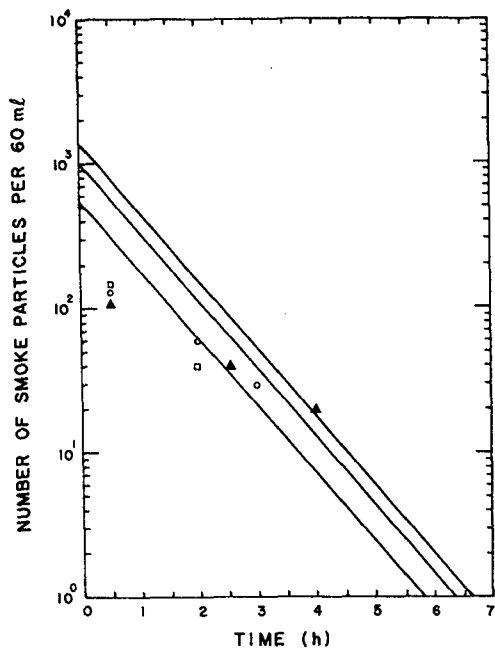


Fig. 12. Evaporation decay for metaldehyde smoke particles determined at -5 C.

When we tried to determine the evaporation curve for -5 C, the fast decay rate at this temperature again caused trouble. Estimation of the initial particle concentration from experiments of lower temperatures, and use of small ice crystal counts detected experimentally, helped determine this decay curve. The -5 C concentration loss curve followed the same evaporation trend as those of lower temperatures. The slopes of evaporation curves are plotted as a function of temperature in Fig. 13. Aerosol

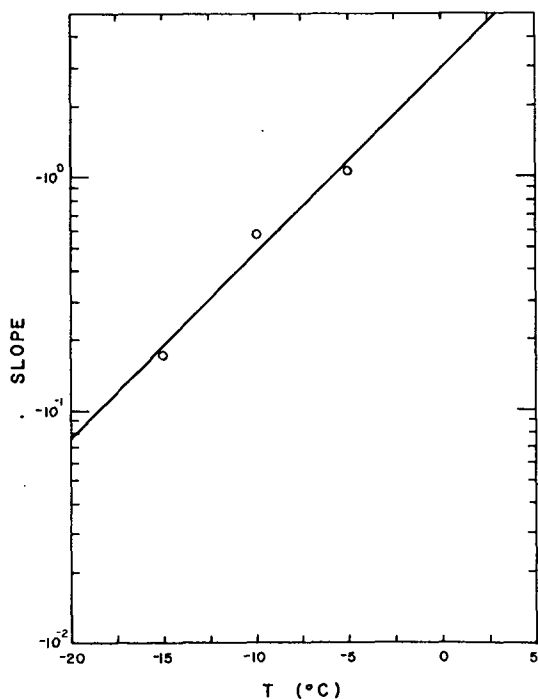


Fig. 13. Slopes of evaporation curves for metaldehyde smoke particles plotted as a function of temperature.

evaporation losses can be calculated for any given temperature using empirical Eq. (7) with $b = 2.978$ and $m = -0.183$.

5. ESTIMATION OF LIFETIME FOR ICE NUCLEUS PARTICLES

To estimate decay of lifetime of organic ice nucleus particles as a function of temperature and size, the activity decay data already obtained must be interpreted with respect to evaporation behavior of the particles in the size distribution curve. Therefore, using the cumulative frequency probability curves representing the aerosol size distribution, and assuming the activity decay proceed from the smaller end of the size distribution because smaller the size, shorter the evaporation lifetime, a relation between nuclei size and decay time for any given temperature can be obtained. To carry out this analysis, the skewed Stokes-Cunningham size spectrum was normalized into a symmetrical distribution (Kottler, 1950), using the log-normal equation,

$$F(d) = \frac{i \Sigma N}{d \sqrt{2\pi} \ln \sigma_g} \exp\left[-\frac{\ln d - \ln M}{2 \ln^2 \sigma_g}\right], \quad (8)$$

where $F(d)$ is the frequency of occurrence of particle diameter d , i the size interval, ΣN the total number of particles in the initial distribution, σ_g the geometrical standard deviation, and M the geometrical mean diameter (Fig. 14). Integration of

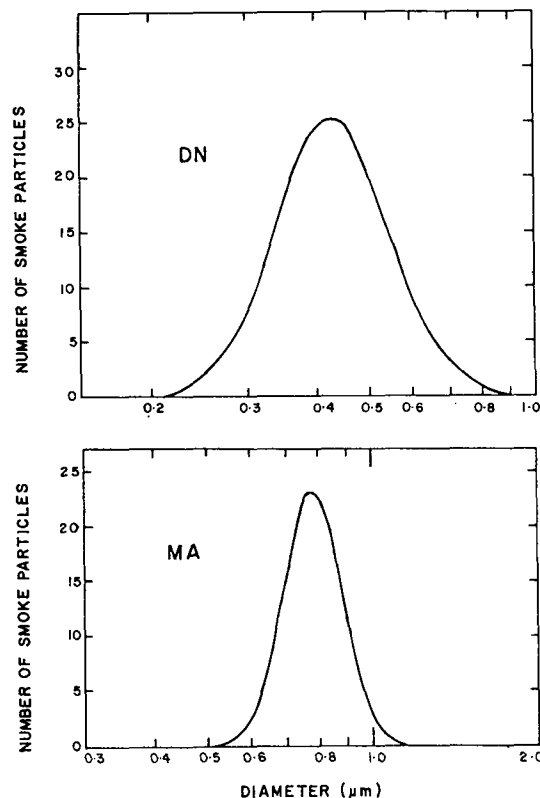


Fig. 14. Log-normal Stokes-Cunningham size distributions for 1,5-dihydroxynaphthalene and metaldehyde smokes.

this function gives the cumulative size distribution curve. Fig. 15 illustrates the cumulative plots for both DN and MA. These graphs reveal, for exam-

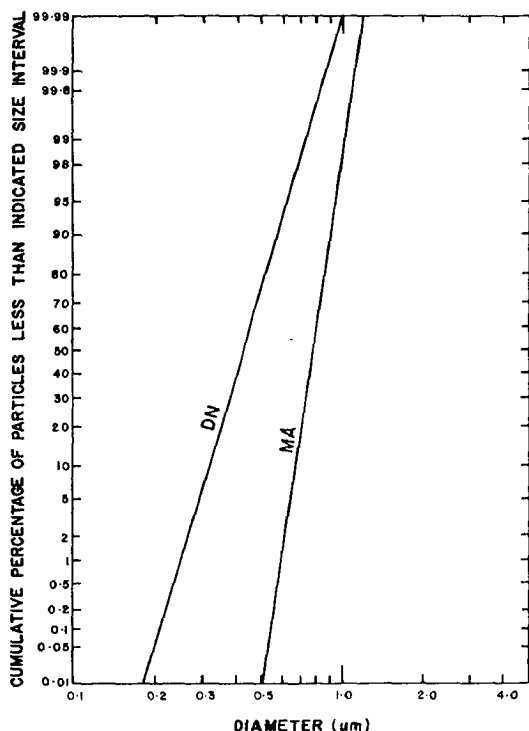


Fig. 15. Cumulative percentage curves plotted as a function of size for 1,5-dihydroxynaphthalene and metaldehyde smoke particles.

ple, that 75% of the total DN aerosol population has diameters smaller than $0.51 \mu\text{m}$, while 90% of MA population is smaller than $0.90 \mu\text{m}$. The percentage of particle activity loss experimentally determined as a function of time can then be correlated with the cumulative percentage distribution in the probability graphs.

5.1 1,5-Dihydroxynaphthalene Particle Lifetime

According to Eq. (7), the percentage of DN aerosol concentration decay as a function of temperature can be determined empirically and then compared, with cumulative size frequency. Figure 16 shows the lifetime of DN particles due to evaporation determined by the above procedure, extended down to representative temperature levels of the real atmosphere. About 90% of the DN aerosol population is analyzed in these results. Since the lifetime of Maxwellian particles is proportional to the square of their sizes, particle evaporation, thus estimated, proceeds very fast for the smaller sizes, especially for those below the detectable size value of $0.17 \mu\text{m}$. Evaporation times are subsequently extended as the size increases

The presence of non-volatile impurities on the particle surface was thought to be responsible for the faster activity decay of small particles, inactivating them as ice nuclei well before complete evaporation. This decay behavior is too complex to predict with the Maxwellian model or the diffusion-kinetic model of constant accommodation coefficients (Fukuta and Walter, 1970). Green and Lane (1964) state that particles of many aerosols are unlikely to evaporate ideally. Non-volatile impurities, formed by slow oxidation or decomposition during evaporation, or even acquired by collision with dust particles, may retard or hinder evaporation.

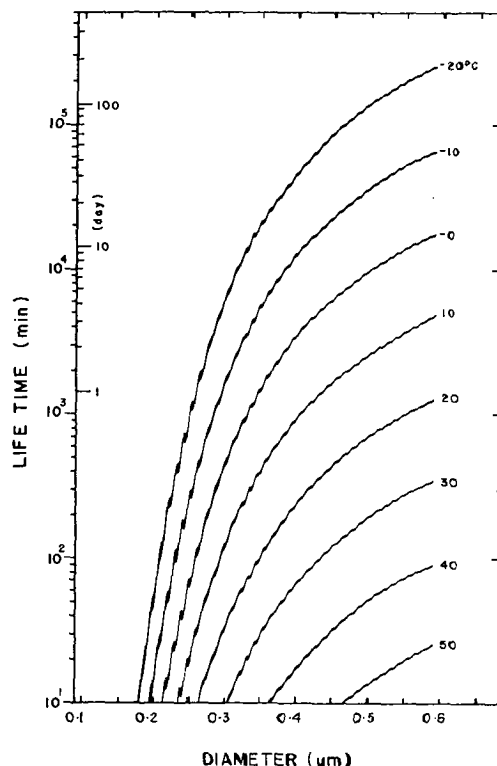


Fig. 16. Lifetime of active 1,5-dihydroxynaphthalene smoke particles estimated as a function of diameter at different air temperatures.

The Maxwellian theory predicts particle evaporation, on the average, six times faster than the experimentally determined rates. Therefore, particle size decay must be estimated graphically. For particles of diameters greater than $0.59 \mu\text{m}$, evaporation times were greatly increased. These few large particles were generally not representative of the remaining distribution, nor of practical use in weather modification, and their slow decay behavior greatly extended the remaining 10% of the evaporation curve. Thus they were not included in these results.

Evaporation of DN particles is strongly temperature dependent. At temperatures warmer than 10 C , less than one day is required for most of the present aerosol to evaporate. Particles exposed to colder atmospheric temperatures would, however, survive longer with possible short-range downwind implications. Experimental and theoretical studies of ice forming nuclei indicate that the optimum cloud seeding particle size is near $0.2 \mu\text{m}$ in diameter, or slightly smaller (Fukuta, 1974). This suggests that reducing DN particle diameter to $0.2 \mu\text{m}$ could shorten lifetime of evaporating DN particles by several days, at temperatures as cold as -20 C .

5.2 Metaldehyde Particle Lifetime

The lifetime for MA particles determined by the same procedure is given in Fig. 17. Evaporation results again represent 90% of the total Stokes-Cunningham size distribution. Particle evaporation is extremely fast for smaller sizes, especially for those below the detectable size of $0.54 \mu\text{m}$. Evaporation rates subsequently decrease, as time and size increase, as in the case of DN. This effect can be interpreted also as the result of non-volatile

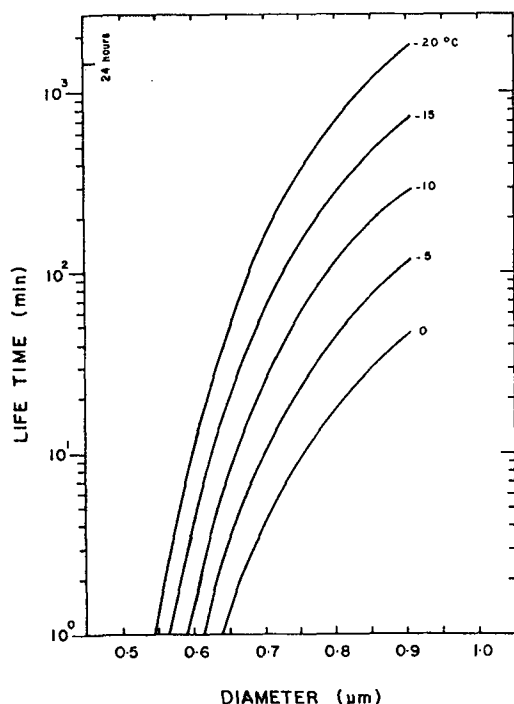


Fig. 17. Lifetime of active metaldehyde smoke particles estimated as a function of diameter at different air temperatures.

impurity accumulation. Slow decay of large particles extended the curve, which were not totally representative of MA particles for cloud seeding use, and hence not plotted. Some 90% of the particles decay within 24 hours, in the temperature range used. According to Green and Lane (1964), aerosol particles of substances with vapor pressures as low as 10^{-4} mb decrease in size perceptibly, which is also recognizable to some degree in our results. MA smoke particles, therefore, not participating in the ice nucleation process, are expected to evaporate quickly and not contribute to any downwind or environmental problems.

Evaporation rates of MA particles can also be calculated from the Maxwellian theory and compared with experimental results. This theory predicted the MA decay rate as considerably faster than that experimentally determined, suggesting retardation mechanisms for evaporation or decay. A continuing shift in size distribution from smaller to larger must therefore occur in the chamber. Hence, evaporation rates for this spectrum can be considered as the slowest possible values, assuming that aerosol particles employed in cloud seeding would be much smaller.

An analytical expression to predict size decay as a function of temperature, vapor pressure, and time, based on either Maxwellian or non-Maxwellian theory, similarly could not be produced. A large difference between size decay predicted by theory and activity loss measured was again noted, and graphical methods had to be employed to estimate the decay behavior of MA (Fig. 17).

6. WEATHER MODIFICATION IMPLICATIONS

As discussed earlier, two of the undesirable effects associated with the current operational weather modification agents include downwind nuclei

contamination, and, to a lesser extent, ecological repercussions. Both environmental problems are directly related to the inability of AgI to decompose under atmospheric conditions. We have estimated the evaporation rates of two potential organic cloud seeding agents, DN and MA, which can provide new insight into when, where, and how to apply these agents to clouds.

We have demonstrated that DN and MA aerosols definitely decay with time through evaporation, depending on particle size and temperature. Particles of MA less than $0.6 \mu\text{m}$ in diameter are shown to evaporate within 20 minutes at temperatures as cold as -20 C (Fig. 17). Particles smaller and more suitable for cloud seeding would definitely produce no undesirable downwind problems. Evaporation of DN is slower, but particles smaller than $0.2 \mu\text{m}$ in diameter should still evaporate and lose activity within a few hours at equally cold temperatures (Fig. 16).

Acknowledgments. This work is based on the M.S. thesis of H.R.V. and was partially supported by the National Science Foundation under Grant ENV 77-15346. This paper was prepared while one of the authors (N.F.) visited the Environmental Research Laboratories of the National Oceanic and Atmospheric Administration under the Senior Academician Program.

7. REFERENCES

- Church, B. D., L. Griffin and J. W. King, 1975: The biodegradability and ecological effects of organic weather modification agents. Final Rept. to N.S.F. under Grant No. GI-33037, Oct. 1975.
- Cooper, C. F. and W. C. Jolly, 1970: Ecological effects of silver iodide and other weather modification agents. A Review. Water Resources Res., **6**, 88.
- Elliott, R. D. and K. J. Brown, 1971: The Santa Barbara II Project-- downwind effects. Proc. Internat. Conf. on Weather Mod., Canberra, Australia, 179 - 183 (Boston, MA, Amer. Meteor. Soc.)
- Fukuta, N., 1963: Ice nucleation by metaldehyde. Nature, 199, 475 - 476.
- _____, 1968: Some remarks of ice nucleation by metaldehyde. Proc. Internat. Conf. on Cloud Physics, Toronto, Canada, August 1968, 522 - 531 (Boston, MA, Amer. Meteor. Soc.).
- _____, 1972: Metaldehyde seeding in summertime cumuli. J. Rech. Atmos., "Memorial Henri Dessens" No. 1-2-3, 165 - 174.
- _____, 1974: Ice nuclei generator technology. J. Weather Mod., **6**, 68 - 78.
- _____, K. J. Heffernan, W. J. Thompson and C. T. Maher, 1966: Generation of metaldehyde smoke. J. Appl. Meteor. **5**, 288 - 291.
- _____, and L.A. Walter, 1970: Kinetics of hydrometeor growth from a vapor-- spherical model. J. Atmos. Sci., **27**, 1160 - 1172.
- _____, L. F. Evans, Y.-H. Paik, W. A. Schmelting, L. A. Walter and T.-L. Wang, 1970: A study of the production and detection of artificial ice nuclei. Final Rept. to Bureau of Reclamation under Contract No. 14-06-D-6444.
- _____, M. N. Plooster, Y.-H. Paik, L. F. Evans, A. Gorove and T. L. Wang, 1973: The engineering, microphysical, and dynamical aspects of precipi-

- tation management. Final Rept. to Bureau of Reclamation under Grant No. 14-06-D-7028, August, 1973
- Fukuta, N., J. Armstrong and A. Gorove, 1975: A new airborne organic ice nuclei generator and its test in summertime cumuli. J. Weather Mod. 7, 17 - 30.
- _____, M. N. Plooster, J. A. Armstrong and J. Butz, 1976: Organic ice nuclei field tests: South Dakota and Leadville Cooperative Projects, Summer, 1975. J. Weather Mod., 8, 67 - 77.
- _____, and Y. Paik, 1976: A supersonic expansion method of ice nuclei generation for weather modification. J. Appl. Meteor., 15, 996 - 1003.
- _____, M. N. Plooster, J. A. Armstrong, A. Gorove, J. A. Butz, R. C. Schaller and L. Glen, 1977: The development of organic ice nuclei generators for weather modification. Final Rept. to N.S.F. under Grant No. ENV 73-02910, June 1977.
- Garvey, D. M., 1975: Testing of cloud seeding materials at the Cloud Simulation and Aerosol Laboratory, 1971-1973. J. Appl. Meteor., 14, 883 - 890.
- Gillispie, T. and G. O. Langstroth, 1951: The aging of ammonium chloride smokes. Canad. J. Chem., 29, 201.
- Grant, L. O. and G. J. Mulvey, 1971: A physical mechanism of extra-area effects from the Climax orographic cold cloud seeding experiment. Proc. Internat. Conf. on Weather Mod., Canberra, Australia, 473 - 479 (Boston, MA, Amer. Meteor. Soc.).
- Green, H. L. and W. R. Lane, 1964: Particulate Clouds; Dusts, Smoke, and Mists, London, E. & F. N. Spon, Ltd., 241 - 244.
- Hesketh, H. E., 1977: Fine Particles in Gaseous Media. Ann Arbor Science Pub. Inc., Michigan, 204 pp.
- Kottler, F., 1950: The distribution of particle sizes. J. Franklin Inst., 250, 339 - 419.
- Schaller, R. C. and N. Fukuta, 1979: Ice nucleation by aerosol particles; Experimental studies using a wedge-shaped ice thermal diffusion chamber. J. Atmos. Sci., 36, 1788 - 1802.
- Sokol, R. A. and D. A. Klein, 1975: The response of soils and soil microorganisms to silver iodide weather modification agent. J. Environ. Quality, 4, 211 - 214.
- Teller, H. L., 1972: Current studies in the ecological effects of weather modification in Colorado. Third Conf. on Weather Mod., Rapid City, N. D., 26-29 June 1972, 226 231 (Boston, MA, Amer. Meteor. Soc.).
- Warburton, J. A., 1971: Physical evidence for transport of cloud seeding materials into areas outside primary target. Proc. Internat. Conf. on Weather Mod., Canberra, Australia, September 1971, 185 - 190 (Boston, MA, Amer. Meteor. Soc.).
- _____, and L. G. Young, 1968: Neutron activation procedure for silver analysis in precipitation. J. Appl. Meteor., 7, 433 - 443.